

Microstructured semiconductor lasers for high-speed information processing

P. L. Gourley

The technology to generate laser light from semiconductor microstructures is developing rapidly. New techniques for epitaxial growth and surface processing allow great flexibility in laser architecture. Highly efficient lasers with submicrometre dimensions, operating independently or packed together in dense two-dimensional arrays, will soon be used for transmitting, storing and manipulating information with unprecedented speed.

IN C. S. Lewis's *The Magician's Nephew*, the world of Narnia began with the creation of lights by the great voice: "the blackness overhead, all at once, was blazing with stars. They didn't come out gently one by one, as they do on a summer evening. One moment there had been nothing but darkness; next moment a thousand, thousand points of light leaped out."

Like the creation of the vast number of stars in Lewis's novel, modern photonics engineers are creating millions of microscopic laser lights on gallium arsenide semiconductor chips. These chips comprise periodic arrays of micrometre-sized lasers emitting coherent visible or near infrared light. These lasers can operate as large arrays or independently to communicate millions of messages at the same time. Such vast numbers of light-emitters could be used to read, write or process two-dimensional images, and to speed the flow of information between memory and processing chips. By replacing cumbersome electronic wires with laser beams, bits of data could move faster between spots on different chips.

Developing semiconductor laser materials use alloys like AlGaAs or other compound semiconductors which emit wavelengths of light extending from 450 nanometres in the blue to 10 micrometres in the infrared. This range covers the wavelengths of the most familiar 'benchtop' lasers such as argon ion (514 nm), YAG (1.06 μm) and CO₂ (10.6 μm). Each of these familiar industrial lasers can produce hundreds of watts of continuous light power. Arrays of the most developed semiconductor lasers, emitting 870-nm light from cleaved GaAs wafers, have demonstrated similar power levels. Discrete semiconductor lasers typically emit from 0.1 mW to 1 W and are the size of a salt grain, many orders of magnitude smaller than benchtop lasers. Semiconductor lasers are clearly the most efficient light sources, with up to 50% overall quantum efficiency, far exceeding efficiencies of the familiar industrial lasers (0.1–0.01%), tungsten lamps (few per cent) and fluorescent arc amps (10%).

Beyond highly efficient light generation, semiconductor lasers are well suited to high-volume manufacturing. Like the integration of silicon transistors in the 1960s, the semiconductor laser will undergo integration in large arrays and with other optical circuit elements such as waveguides and detectors. The ultimate uses of optical circuits are still an open question. But it is likely that information display and transfer, energy delivery and computation are among the leading applications. As these applications become a reality, our society will be more dependent on new materials for photonics.

Three-dimensional architectures

Many technological advances are inherited from the new geometries of microstructured semiconductor lasers¹. These new forms have emerged through modern semiconductor microfabrication, including epitaxial growth and surface processing. Such technologies allow the creation of three-dimensional laser architectures that enhance light emission from the materials used to build them.

Several advantages follow from the microstructure inherent in the crystalline growth of the laser crystal. The crystal is literally built up atomic layer by atomic layer onto a semiconductor substrate by epitaxy. Techniques like molecular beam epitaxy and metal organic vapour-phase epitaxy allow sequential layering of hundreds of different semiconductor alloys. By mixing and matching these 'designer materials', crystals can be layered together to optimize the electrical and optical properties. This tailoring of semiconductor structures is called bandgap engineering, and is described below.

Every semiconductor has an energy gap that separates lower-energy, occupied electron states (valence bands) from the higher-energy, empty states (conduction bands). An electron promoted across this gap will result in a mobile 'hole' in the valence band and a mobile electron in the conduction band. In bandgap engineering, different semiconductor alloys with different bandgaps are joined during growth to form a single-crystal heterojunction. This heterojunction creates potential-energy steps in conduction and valence bands that inhibit motion of electrons and holes. A double heterojunction with a thin layer (~ 100 Å) of low-bandgap material (such as GaAs) sandwiched between two wide-bandgap materials (such as AlGaAs) is called a quantum well (Fig. 1 shows a three-quantum-well structure); in these structures, used in most semiconductor lasers, individual electrons and holes are confined within the central layer.

An alternative, thicker heterostructure is an optical waveguide layer, in which a thick ($\sim 1,000$ -Å) GaAs layer is sandwiched between two AlGaAs layers. Light is guided by total internal reflection along the GaAs layer because it has a higher refractive index than AlGaAs.

Another important heterostructure is a quarter-wave mirror stack, sometimes called a distributed Bragg reflector. It comprises periodic pairs of layers (GaAs and AlAs, for example) with high and low refractive index to reflect light incident perpendicular to the layer (Fig. 1). The waves of light reflected from each interface add constructively to create a very high reflectance exceeding 99%. The individual layer thicknesses d correspond to a quarter wavelength of light, $d = \lambda/4n$ where λ is the wavelength and n the refractive index. For GaAs $n = 3.6$ at the emission wavelength of $\lambda = 850$ nm, so $d = 630$ Å.

With epitaxial growth, these building blocks (quantum wells, optical waveguides and mirrors) can be stacked in a single crystal according to a designer's wishes. After growth, the surface of the crystal wafer can be patterned by optical or electron-beam microlithography using a spin-on resist material. After the resist is exposed and developed, selected areas as small as a few tens of nanometres can be removed from the wafer's surface by etching techniques. These techniques use 'wet' chemicals or 'dry' ion beams to strip off layers with nearly the same precision as they were laid down.

Taken together, epitaxial layering and surface processing allow the photonics engineer great flexibility in the geometry of

lasers. Developing semiconductor lasers exhibit an astonishing variety of geometrical forms including multilayer sandwiches^{2,3}, posts⁴, gridirons⁵, thumbtacks⁶, swiss cheese⁷, concentric rings⁸ and honeycombs⁹. A checkerboard geometry¹⁰ for a phase-compensated two-dimensional surface-emitting laser array is shown in Fig. 2a. The pattern of light emitted from an uncompensated array is shown in Fig. 2b and c, for the near and far fields respectively.

Vertical-cavity surface-emitting lasers

Although many microstructured lasers are still in their infancy, others are more developed. The vertical-cavity surface-emitting laser (VCSEL) (Fig. 1) is now making the transition from research to manufacturing. This structure includes all the necessary laser components: optical cavity, gain medium and electrical pathway for current, built within a single-crystalline architecture. It comprises three basic components: an n-type mirror for conducting electrons, a p-type mirror for conducting positively charged holes, and a central quantum-well active region. The mirrors define an optical cavity that confines photons for the lasing process.

The general operation of a semiconductor laser can be explained with Fig. 1. With a low voltage (a few volts) applied, electrons flow from the leftmost metal contact through the substrate and n-type mirror to quantum wells, where they collect. At the same time holes are injected through the rightmost metal contact, through the p-type mirror, and into the thin quantum wells. When an electron encounters a hole in the quantum well, the pair is annihilated (or recombines) and a photon is produced. The light produced by this chance encounter is called spontaneous emission. Spontaneous photons are randomly emitted in all directions and are frequently reabsorbed by the quantum well materials. Spontaneous emission tends to be weak and have a broad energy distribution.

When the bias voltage is increased, dramatic changes take place. Increased flow of electrons and holes fills the energy states of the quantum wells and optical gain is developed. In this condition, a spontaneous photon traversing the quantum wells will induce another electron-hole recombination event and photon emission (stimulated emission). These stimulated photons multiply the photon population many times. Only those waves which reinforce themselves after a cavity roundtrip with two mirror bounces will build up. These stimulated photons add constructively to produce an intense standing wave in the cavity. In the steady state, some of the stimulated photons leak out through the mirrors, producing a coherent, monochromatic beam outside the cavity.

Bandgap engineering of the vertical-cavity laser structure has evolved over the last fifteen years^{2,3,11-23}, following the pioneering work by Iga of the Tokyo Institute of Technology². Most of the pioneering VCSEL diode work has been accomplished with the GaAs/AlGaAs materials that emit in the near infrared (770-1,000 nm). Recent advances include demonstration of AlGaInP-based visible (red at 650-670 nm) VCSELs (Fig. 3)²¹, and InGaAsP-based VCSELs operating at 1.3 μm . Newly developed compound nitride semiconductors may even allow short-wavelength VCSEL lasers emitting in the ultraviolet-blue region of the spectrum.

Advantages of microstructured lasers

The vertical cavity of Fig. 1 is versatile; it can be used for light generation^{2,3}, modulation²⁴ or switching^{25,26}. As a laser, it can

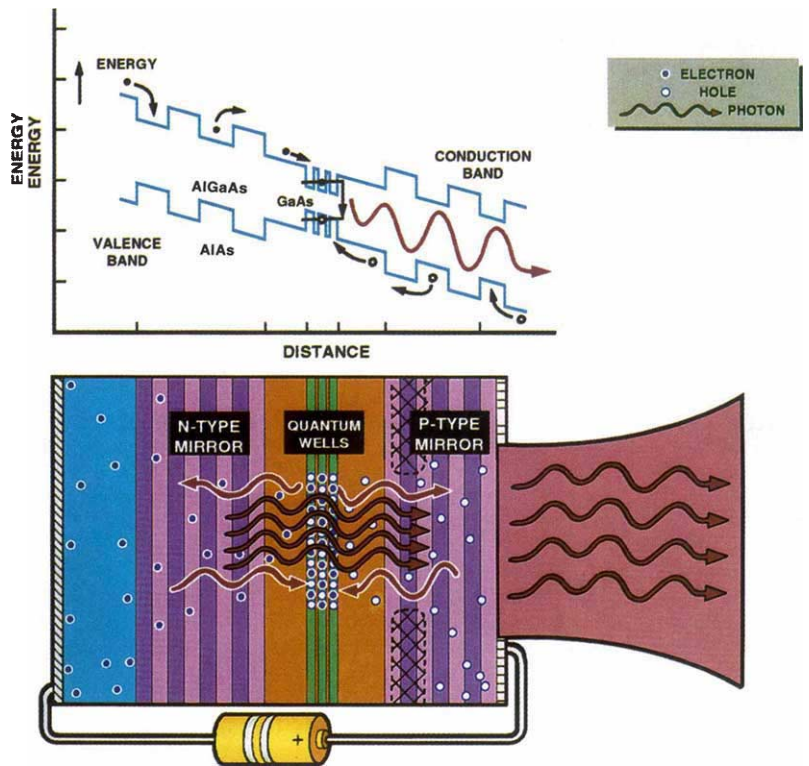


FIG. 1 Diagram of a single vertical-cavity surface-emitting laser. The upper part shows the conduction and valence bands in which the electrons and holes move. The bottom part shows the layered pairs of semiconductor materials used for the mirror region and thinner quantum-well layers used in the active region. Electrons and holes are shown by dark and open circles respectively. These carriers are injected from metal contacts applied to the substrate and top mirror layer. The carriers collect into the quantum wells where they recombine to produce photons (wavy arrows). Photons with the right wavelength are multiplied inside the laser cavity. Some of these photons leak out the top mirror, through an aperture defined in the top metal contact, to produce an intense beam.

operate as a planar device, etched post or two-dimensional array. Its architecture is radically changed from the conventional edge-emitting laser invented in the early 'sixties. In contrast to that laser, which emits widely diverging light from a cleaved wafer-edge, the vertical-cavity laser emits light normal to the wafer surface. This allows vast numbers of lasers to be packed side-by-side on the wafer surface or to be integrated vertically with other optical elements. It also allows the laser aperture to shape the emerging beam into a low diverging circle, compatible with fibre optics. The circular beam cross-section of a VCSEL is contrasted with the stripe-like beam from an edge-emitter in Fig. 3.

The advantages of bandgap engineering are illustrated by a recent scheme to lower the electrical resistivity of VCSEL mirrors. The quarter-wave stack must serve three functions: as a highly reflecting mirror, as a conducting path for charge carriers and as a sink to remove unwanted heat. These three requirements are not generally compatible, but can be accommodated by bandgap engineering. For the first function, large differences in the indices of refraction of adjacent mirror layers give high reflectivity. Large index differences are accompanied by large energy barriers, which charge carriers must surmount as they move across layers. These barriers impede carriers, causing high resistances which create heating and lower efficiency. To lower the resistance but maintain high reflectivity, the interfaces between layers are graded in alloy composition to 'soften' the energy barrier. A grading approach developed at Sandia²⁷ and at the University of California at Santa Barbara²⁸ have produced low-resistance mirrors enabling VCSEL threshold voltages of less than 1.5 V and efficiencies of up to 30%.

The laser benefits from bandgap engineering of the active region. The quantum wells can be placed commensurately with

FIG. 2 *a*, Scanning electron micrograph of a two-dimensional vertical-cavity surface-emitting laser array with integrated phase compensator made at Sandia National Laboratories by Warren and co-workers. The individual laser pixels are 5- μm squares with every other pixel covered with a glass-shifting layer. *b*, The near field laser light emitted from an uncompensated 20×20 array injected with current. *c*, The four-lobed light pattern observed far from the device surface (far field).

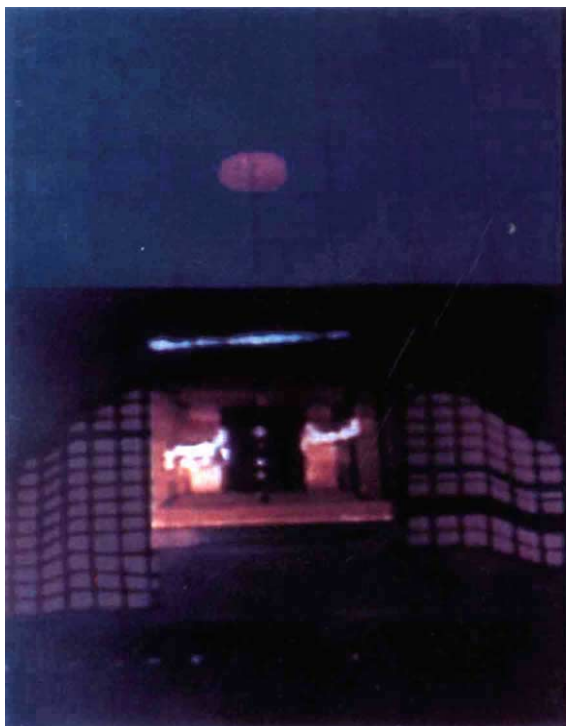
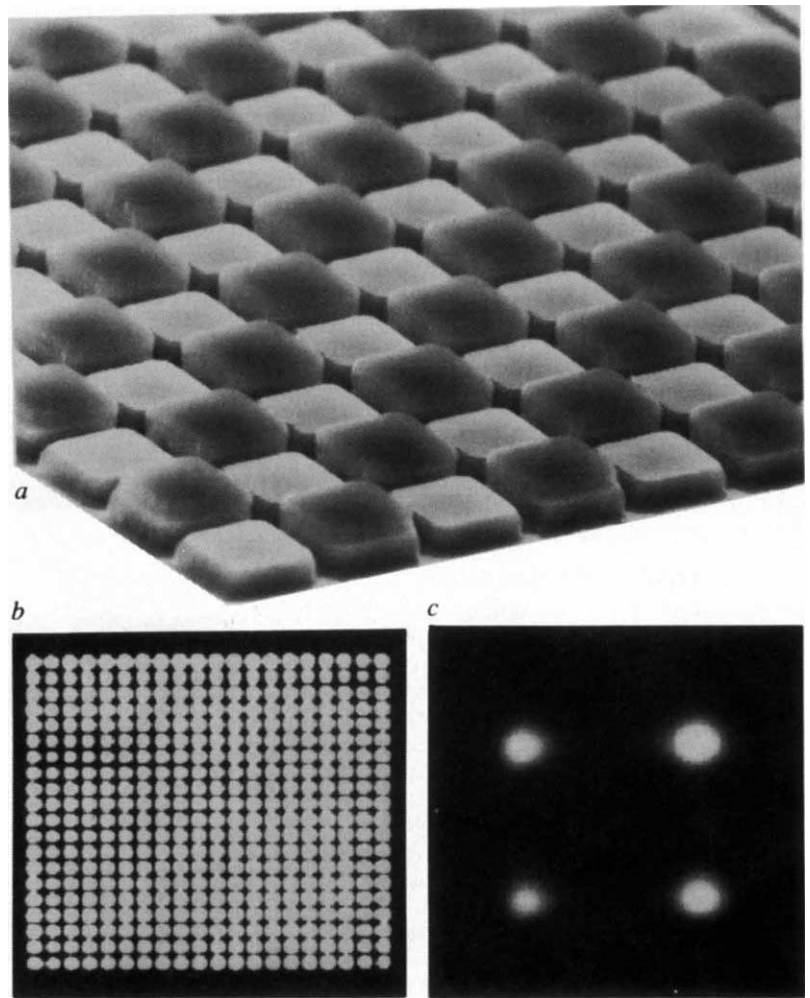


FIG. 3 Cross-sections of visible laser beams from a new surface-emitting laser diode (left) contrasted with conventional edge-emitting laser diode (right). The red beam from the surface-emitter illuminating the backside of a paper screen is

circular and much smaller than the wide, stripe-like beam from the edge-emitting laser. These properties simplify the collimation and focusing of the VCSEL. (Photographs courtesy of R. Schneider and K. Lear of Sandia National Laboratories.)

the antinodes in the optical standing wave²⁹⁻³¹. This effect is illustrated in Fig. 1 where the crest in the optical waves aligns with the quantum wells. The lasing wavelength is stabilized, the gain material is more effectively utilized to feed the lasing process, and evidence suggests that spontaneous emission is enhanced^{32,33}. The quantum wells can be thin elastically strained layers, to extend lasing wavelength and increase efficiency³⁴⁻³⁸. Furthermore, the ultra-short active region can be designed to improve temperature characteristics^{39,40} and increase the upper frequency (~ 14 GHz) for switching the laser on and off⁴¹⁻⁴⁵.

Beyond performance characteristics, the vertical-cavity surface-emitting-laser is particularly attractive for manufacturing. VCSELs can be individually tested while they are still in wafer form. Because defective lasers are identified before packaging, costs are reduced. The surface emission geometry of VCSELs will also simplify packaging.

Surface-patterned laser arrays

Whereas layered microstructure is used to enhance the efficiency of the lasing process, surface microstructure is used to shape and direct the beam emitted from the wafer. Surface patterning is useful for creating two-dimensional arrays of surface-emitting lasers. When many of these tiny lasers are placed side by side on a wafer, it is possible to operate them in a phase-locked condition (Fig. 2*b*). As a consequence, the entire array operates in unison to create a narrow laser beam. By adjusting the relative phase of the lasers, it may even be possible to steer the beam in space at very high speed.

The lasing modes in a two-dimensional arrays have been studied recently^{5,10,46-51}. The optical mode in the array will determine the angular distribution of light observed far from the array surface (far field). The far-field patterns observed experimentally reveal four bright spots (Fig. 2*c*). The spots are placed symmetrically 5° away from the optical axis into each of the four quadrants of the far field. The width of the spots (θ) is about 2° , slightly broader than predictions of $\theta \approx \lambda/D$ by diffraction theory, where D is the diameter of the array. The surface-patterned array has a beam with much lower divergence than that of a single element of the array.

Despite the advantages of narrower divergence, the beam intensity is off the optical axis (normal to wafer surface). Most applications require a single beam on the optical axis. The off-axis beam is due to the array mode which corresponds to each element being 180° out of phase with its neighbours. This antisymmetric mode dominates the lasing process. The mode amplitude has a zero crossing between elements, consistent with the quenching of lasing in the channels. Attempts have been made to produce a symmetric mode with on-axis intensity, but with little success.

A more successful approach taken by Warren and co-workers is to let the array lase in its preferred antisymmetric mode and then use epitaxial binary optics to adjust the phase in the near field^{10,49}. In this case, an extra phase-correction layer is grown above the top mirror. After growth, the layer is selectively removed above every other lasing element. This leaves a checkerboard pattern etched into the phase-correction layer (Fig. 2). In the squares with remaining material, the phase of the outgoing wave is retarded by 180° with respect to the squares without the material. The phase front of the wave is now compensated across the entire array surface, as if the array was operating in a symmetric mode. The far-field pattern comprises a bright lobe on

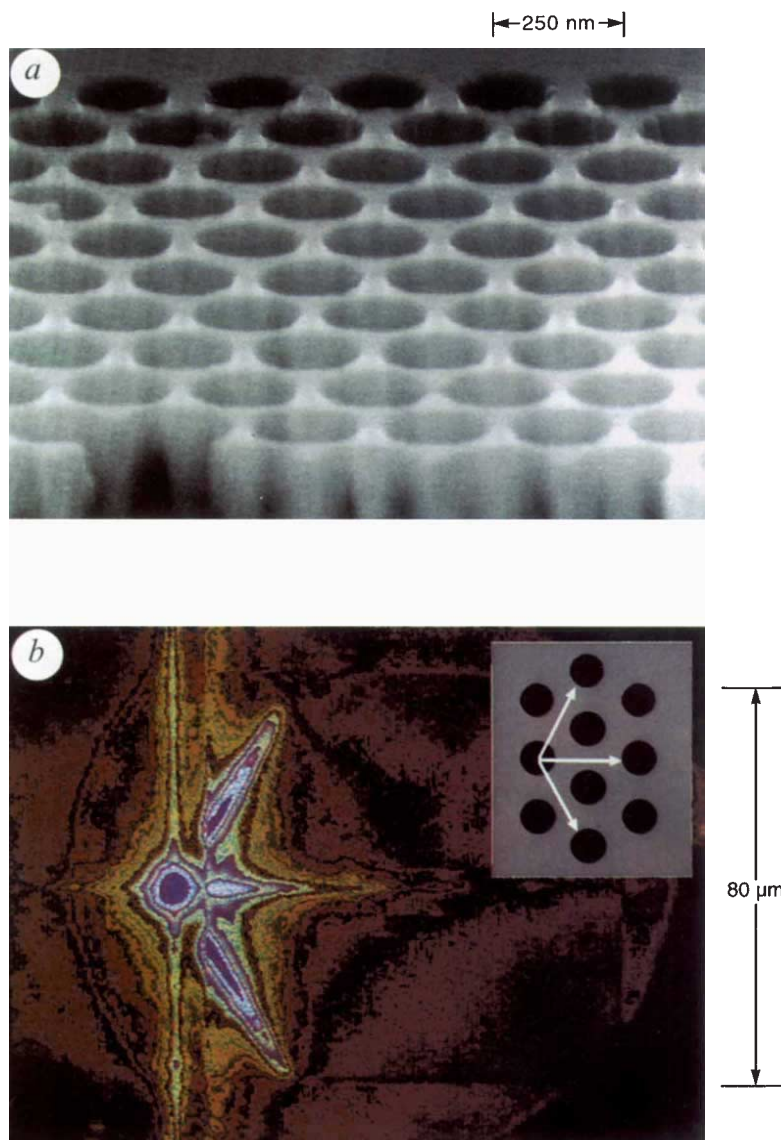


FIG. 4 *a*, Scanning electron micrograph of a photonic lattice structure fabricated with electron beam lithography and reactive ion beam etching by Wendt and Vawter at Sandia National Labs. The structure features 250-nm diameter holes etched into a AlGaAs multilayer wafer. Photonic lattices such as this one are being investigated for future generations of low-threshold lasers. *b*, A light scattering micrograph showing how light propagating along the wafer plane is redirected out of the plane by the lattice.

the optic axis as desired. There are also secondary lobes off the optical axis, but these are weaker.

Photonic lattices and band gaps

The above example shows how surface patterning of an epitaxial layer can be used to produce a phase transformation in a wave exiting the crystal. A slight phase adjustment in the near field produces a dramatic change in the far field, which is its Fourier transform. Study of the far field can provide valuable information about the optical modes in the arrays⁵⁰. These arrays form a subset of more generalized periodic optical structures called photonic lattices. A photonic lattice is formed by periodic modulation of the dielectric constant (or refractive index) in one, two or three dimensions. The distributed Bragg reflector is a one-dimensional photonic lattice. Lattices of all dimensionalities serve to inhibit the propagation of electromagnetic radiation over a range of frequencies called a stop band. A stop band in three dimensions could entirely prohibit spontaneous emission. These effects would be useful for laser cavities, waveguides and detectors.

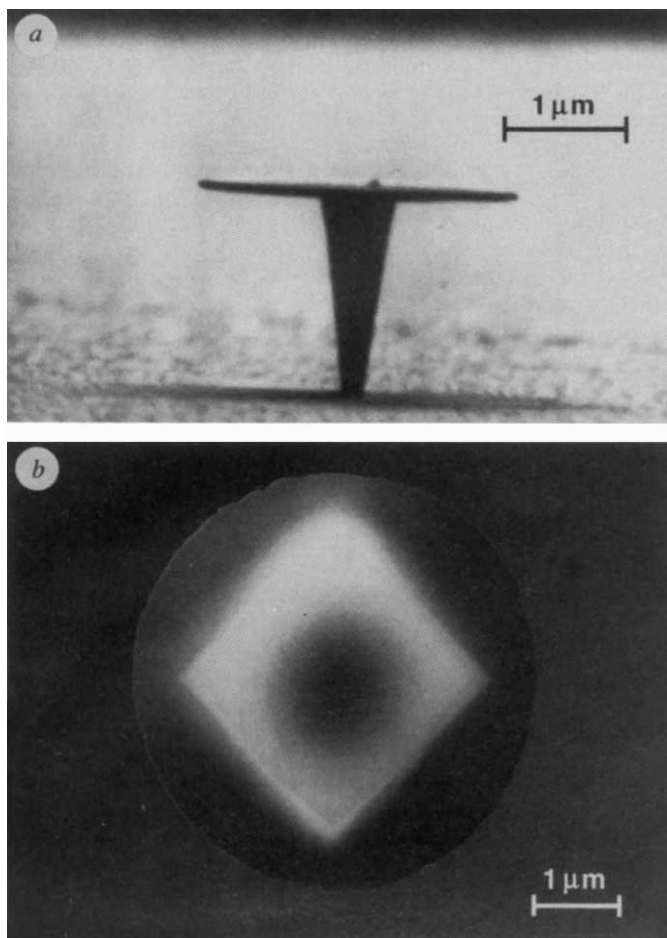


FIG. 5 Scanning electron micrographs of microdisks in the side view (a) and top view (b). The InP pedestal is a rhombus in cross-section as seen in the top view. It tapers to smaller dimensions as it approaches the substrate. (Photograph courtesy of R. Slusher of AT&T Bell Laboratories.)

Optical waves in the lattice are analogous to electron Bloch wavefunctions in a crystalline solid⁵²⁻⁵⁵. The electron wavefunction in the solid is described by local orbital motion around each atom and by long-range wave motion throughout the periodic arrangement of atoms. When the electron wavelength is twice the atomic spacing, the Bragg condition for reflection occurs. Under this condition, the electron wave cannot propagate,

creating the energy bandgap described earlier in this article. In the photonic lattice the stop band corresponds to the energy bandgap. Like electrons, the photons can exist in energy states where propagation is allowed. Unlike electron states which accommodate one electron at a time, the photon states can accommodate many photons at a time. These differences endow the photonic lattice with unusual properties, useful for nonlinear optics and not found in electronic lattices.

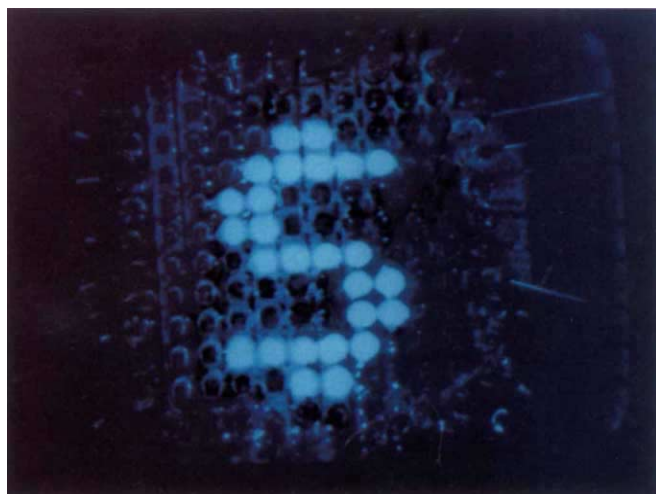
Recently, specific three-dimensional photonic crystals have been proposed by Yablonovitch⁵⁶ and others⁵⁷⁻⁶⁰. These structures are being intensely studied theoretically by many groups. This work has shown that complete three-dimensional photonic bandgaps are possible for certain crystal symmetries with sufficient dielectric modulation. Experimentally, the situation is much less developed. Experiments performed at microwave frequencies have confirmed the existence of photonic bandgaps in two dimensions (posts in triangular arrays⁶¹) and three dimensions (stacked-log structures operating up to 500 GHz^{62,63}) using insulators or semiconductors. Structures with bandgaps in the optical frequencies have proven difficult to make because of the small submicrometre dimensions necessary.

It may be easier to make two-dimensional structures with photonic bandgaps at optical frequencies. Two-dimensional lattices which have a complete in-plane photonic bandgap have been theoretically predicted by Meade *et al.*⁶⁴ and Villeneuve and Piche⁶⁵. Honeycomb lattices and triangular lattices of air holes have a complete gap for both transverse electric and transverse magnetic polarizations. The maximum bandgap occurs in structures with ~85% air-volume fraction. Honeycomb nanostructures have been fabricated by Wendt and Vawter at Sandia National Laboratories⁹. These structures, (Fig. 4a), were fabricated in compound semiconductors using electron-beam lithography and reactive-ion-beam etching. The honeycomb nanostructure corresponds to two-dimensional second-order Bragg-reflector wavelengths near 830 nm. This includes wavelengths for the spontaneous emission from GaAs quantum wells. Initial optical characterization of these lattices reveals that light normal to the plane can be resonantly coupled into the lattice near the Bragg condition⁹. A photomicrograph of light propagated and scattered out of the lattice is shown in Fig. 3b. The image shows that the lattice is effective in controlling the direction of photon propagation.

Whispering-gallery microdisk lasers

One major hurdle for semiconductor lasers is the elimination of the heat that accompanies light generation. To obtain high operating efficiencies, considerable energy must be expended to overcome the threshold condition for inverting the electron populations in order to start the lasing process. This threshold

FIG. 6 A 850-nm light display from a 10×10 matrix addressable array fabricated at the Solid State Technology Center of AT&T Bell Laboratories. Matrix addressing has the advantage of minimizing the number of wires to inject current. The dollar-sign display is created by raster scanning the array to turn individual elements on and off. These arrays are proposed for applications such as video imaging, confocal microscopy and spatial light modulation. (Photograph courtesy of R. Morgan, formerly with AT&T Bell Laboratories and now with Honeywell.)



condition might be compared to the heat required to raise the temperature of a pot of water to produce boiling. If the pot were made small enough and the energy supplied without loss, the threshold energy for boiling could be very low. How to make such a 'thresholdless laser', suggested by Yamamoto⁶⁶, is a topic receiving much attention. Such a device would operate at the quantum limit: the first injected electron-hole pair would produce a laser-like photon. One approach to implementing this laser uses a photonic lattice⁹ (Fig. 4a).

Other approaches to confine light for thresholdless lasers are also being investigated⁷. These approaches include fabrication of vertical-cavity posts, hemispherical cavities and whispering-gallery disks⁶. The object is to make small high-quality-factor microcavities to localize a few modes from the surrounding free-space modes. If the cavity is small enough, it can even modify the spontaneous emission rate of photons. Useful spontaneous emission can be enhanced and competing emission can be suppressed. The result is that device quantum efficiency increases. Like vertical cavities, these structures feature single-mode lasing, high-wavelength stability and low temperature-sensitivity. Ultrasmall cavities may even produce photon number squeezing, where the emitted photon stream is highly correlated in time and does not obey Poisson statistics. Theorists are now thinking of schemes to produce a correlated flow of electrons to inject such a microcavity.

A measure of merit for these microcavities is the fraction of spontaneous emission that is coupled into the lasing mode (β). β can also be interpreted as the inverse of the number of optical modes in the cavity. As β approaches 1, the threshold current for lasing decreases, the lasing linewidth narrows, and the laser intensity fluctuations decrease⁶⁶. An approximation for the spontaneous emission coefficient at wavelength λ is $\beta \approx (\lambda/2n)^3 \lambda / V \Delta\lambda_{sp}$ where $(\lambda/2n)^3$ is the optical volume per mode, V is the total cavity volume and $\Delta\lambda_{sp}$ is the linewidth of the spontaneous-emission spectrum. Large-area vertical-cavity surface-emitting lasers have $\beta \approx 0.01$. Posts etched into these laser wafers have $\beta \approx 0.1$. Even higher values ($\beta \approx 0.3$) are attained with 'whispering-gallery' microdisk lasers⁶. The values in photonic lattices and photonic bandgap materials are expected to approach 1, but have not yet been demonstrated experimentally.

A scanning electron micrograph of a 'whispering-gallery' microdisk laser is shown in Fig. 5. These microdisks were fabricated by etching quantum-well layers of InGaAs/InGaAsP (100 Å well/100 Å barrier) grown on InP substrates. The total thickness is 500 Å for a single-quantum-well structure and 1,500 Å for a six-quantum-well structure. Photolithography was used to pattern cylinders with diameters of 3–10 μm. A hydrochloric acid solution was used to etch away the InP around and below the protected circles, leaving a very thin quantum well/barrier disk. The disk is mechanically stable and lases when optically or electrically pumped.

These microdisk lasers are simple to make and attractive for several reasons. First, the disk volume is extremely small, only 1 μm³. This is about 100 times smaller than a vertical-cavity laser. Consequently, the current required for lasing is very low, in the microamp range. Second, the refractive-index mismatch between the semiconductor disk ($n=3.6$) and surrounding air ($n=1$) is enormous. This leads to very high confinement of spontaneous or stimulated photons created inside the disk. Only a single transverse optical mode is trapped in the thin disk. Third, the photons tend to skim along the circumference of the disk where they experience total internal reflection as in an optical waveguide. This gives very high overlap between the optical wave and gain present in the quantum wells, allowing the laser to operate more efficiently.

The optical waves in these disks are referred to as 'whispering-gallery' modes, analogous to sound waves first observed by Lord Rayleigh. More than a century ago, he explained how conversations could be heard at opposite walls inside the great dome of St Paul's Cathedral in London. The conversation was channelled

to the listener by efficient propagation of sound waves skimming along the walls. Similar optical waves have been observed in polymer spheres and water droplets. Light can be highly confined within these microstructures because of the high index mismatch between the sphere and its surroundings.

Although light is tightly confined in microdisk lasers, sufficient leakage occurs through the sides to form an output beam. The output power ranges from tens to hundreds of microwatts. The light emitted from a 5-μm microdisk is spread into a ~20° angle about the circumference of the disk. Exactly how to best utilize this circular spread of light is a topic of high interest. The most useful output may emit from an array of microdisks, or from microdisks that are specially positioned to reflect light from the substrate.

As microdisks and other laser structures shrink to smaller and smaller dimensions, physicists are becoming especially intrigued by fundamental limitations on laser operation. The electron, photon and phonon (lattice vibrations) states change from continuous distributions to discrete levels separated by large energies. Electrons and holes injected into such structures find fewer degrees of freedom to relax excess energy. As a result, the energy distribution of carriers is 'hot' and spread over a large range of energies. This energy spreading lowers the conversion efficiency of an injected electron-hole pair into a lasing photon. These limitations will present new challenges for scientists and engineers to overcome.

Quantum-cascade lasers

The emission wavelength of most semiconductor lasers is fixed by the energy bandgap of the quantum-well material in the active region. The laser wavelength is $\lambda = hc/E_g$ where h is Planck's constant, c is the speed of light in a vacuum and E_g is the energy gap between electrons in the conduction band and holes in the valence band. Recently, a fundamentally new microstructured semiconductor laser^{67,68} has been demonstrated by Capasso and co-workers at AT&T Bell Laboratories which removes this constraint. This new laser, dubbed the quantum-cascade laser, has its wavelength set, not by the bandgap, but by smaller energy separation of conduction sub-bands in adjacent quantum wells of different thickness. Since the sub-band energies change with quantum-well thickness, the lasing wavelength can be changed merely by growing thicker or thinner quantum-well layers. Using 8-Å and 35-Å InGaAs well-layers sandwiched between 35-Å AlInAs barrier layers, the demonstration laser emitted light at 4.2 μm in the infrared. Lasers operating at wavelengths of 4–100 μm, appropriate for environmental monitoring and analytical spectroscopy, should be possible with different layer thicknesses.

This remarkable new laser relies on bandgap engineering to accomplish this feat. It was produced by molecular beam epitaxy of 500 layers of variously doped semiconductor alloy layers to define the quantum-well active region, waveguide cladding layers and top contact layer. The laser light travels along the layers in a waveguide and out-edge mirror-facets formed by cleaving the wafer. This lasing direction is similar to conventional edge-emitting laser diode light.

In contrast to both edge- and surface-emitters, this new laser is not a diode. In the diode lasers both electrons and holes are required for recombination events to produce photons. In the quantum-cascade laser only electrons in the conduction band are required. The electrons are injected over a barrier layer where they pile up in the narrow 8-Å InGaAs layer. The electrons cascade downward in energy to the 35-Å InGaAs layer by emitting a 4.2-μm photon. After releasing this energy, they are quickly swept away into adjacent layers. The rates of injection, photon emission and sweepout are carefully regulated by design of the bandgap-engineered layers. This careful regulation is necessary to maintain a population inversion of electrons between the energy levels of the narrow and wide InGaAs quantum-well layers, so the stimulated emission process can take place.

With stimulated emission, up to 8 mW output power at cryogenic temperatures was reported. It is likely that higher output power and operating temperature will be achieved in succeeding laser designs. The implications of mid-infrared to submillimetre-wavelength lasers based on wide-bandgap, technologically mature compound-semiconductor alloys are apparent. Low-bandgap materials for longer wavelength edge-emitting diodes are difficult to grow, hard to process and highly temperature-sensitive. The quantum-cascade laser materials are compatible with those used for long-wavelength infrared detectors based on optical absorption between quantum-well sub-bands. No p-n junction is required, so difficulties associated with p-type doping and hole transport are eliminated. Further, the temperature dependence of the threshold current is predicted to be much weaker than that in diode lasers.

Applications of microstructured lasers

As researchers continue to develop new microlasers with smaller volumes and higher β , manufacturers are scaling up to produce the more developed VCSEL lasers for several different applications. American manufacturers include Motorola, Photonics Research Incorporated and Optical Concepts. One application of interest, a matrix addressable array display⁶⁹ developed at AT&T Bell Laboratories, is shown in Fig. 6. For fibre-optic communications, these lasers feature high coupling efficiency to fibres, low bit error rate, low temporal dispersion and a threshold current that is insensitive to changes in temperature. Such VCSEL applications are under investigation by the ARPA sponsored Optoelectronics Technology Consortium (OETC)

which includes AT&T, GE, Honeywell and IBM. The OETC is working towards a 32-channel, 500-Mb s⁻¹ optical data link for board-to-board communications⁶⁹. The red VCSEL is also an excellent candidate for use in printing, read/write and scanning applications such as a replacement for He-Ne lasers in super-market bar code scanners. Reprographic films are more sensitive at red wavelengths, and the circular beam simplifies focusing light on the film. Plastic micro-optics can be integrated with the lasers, resulting in low-cost miniature laser systems. Finally, two-dimensional VCSEL arrays are particularly attractive for a wide variety of image processing and optical computing applications.

An unprecedented capacity to synthesize microstructures is changing the form of the semiconductor laser. The ability to confine single optical modes in submicrometre-sized lasers in a single crystal is also changing the way we think about semiconductor lasers. It is possible to envisage extremely high-confinement resonators occupied by single photons. Low quantum occupation would allow entirely new kinds of photonic devices using minute power. These devices could become viable system components for transmitting, storing and manipulating information. The conception, fabrication and study of these device structures is creating new opportunities and exciting new challenges for scientists and engineers. Vertical-cavity surface-emitting lasers have already moved toward the manufacturing stage. They are compact, efficient and relatively inexpensive to manufacture in large quantities. The future of these tiny lights appears to be very bright indeed. □

P. L. Gourley is at Sandia National Laboratories, Albuquerque, New Mexico 87185, USA.

1. Yamamoto, Y. & Slusher, R. E. *Physics Today* **46**, 66–73 (1993).
2. Iga, K., Koyama, F. & Kinoshita, S. *J. Quantum Electron.* **242**, 1845–1855 (1988).
3. Gourley, P. L. & Drummond, T. *J. Appl. Phys. Lett.* **50**, 1225–1227 (1987).
4. Jewell, J. L., Scherer, A., McCall, S. L., Gossard, A. C. & English, J. H. *Appl. Phys. Lett.* **51**, 94–96 (1987).
5. Gourley, P. L. et al. *Appl. Phys. Lett.* **58**, 890–892 (1991).
6. McCall, S. L., Levi, A. F. J., Slusher, R. E., Pearson, S. J. & Logan, R. A. *Appl. Phys. Lett.* **60**, 289–291 (1992).
7. Yablonovitch, E., Gmitter, T. J. & Leung, K. M. *Phys. Rev. Lett.* **67**, 2295–2298 (1991).
8. Erdogan, T., King, O., Wicks, G. W., Hall, D. G., Dennis, C. L. & Rooks, M. J. *Appl. Phys. Lett.* **60**, 1773–1775 (1992).
9. Gourley, P. L., Wendt, J. R., Vawter, G. A., Brennan, T. M. & Hammons, B. E. *Appl. Phys. Lett.* **64**, 687–689 (1994).
10. Warren, M. E. et al. *Proc. SPIE OE/LASE Conf.*, Los Angeles, 1994 (Society of Photo-instrumentation, Bellingham, Washington DC, 1994).
11. Van der Ziel, J. P. & Illegems, M. *Appl. Opt.* **14**, 2627–2629 (1975); **15**, 1256–1258 (1976).
12. Gibbs, H. M. et al. *Appl. Phys. Lett.* **41**, 221–223 (1982).
13. Gibbs, H. M. in *Optical Bistability: Controlling Light with Light* (Academic, New York, 1985).
14. Guy, D. R. P., Apsley, N., Taylor, L. L. & Bass, S. J. *SPIE* **792**, 189–193 (1987).
15. Miller, D. A. B. *IEEE J. Quantum Electron.* **QE17**, 306–313 (1981).
16. Ogura, M., Hata, T., Kawai, N. J. & Yao, T. J. *Appl. Phys. Japan* **22**, L112–L114 (1983).
17. Jewell, J. L. et al. *Electron. Lett.* **25**, 1123–1124 (1989).
18. Lee, Y. H. et al. *Electron. Lett.* **25**, 1377–1378 (1989).
19. Lee, Y. H., Tell, B., Brown-Goebeler, K., Jewell, J. L. & Hove, J. V. *Electron. Lett.* **26**, 711–712 (1990).
20. Geels, R. S., Corzine, S. W., Scott, J. W., Young, D. B. & Coldren, L. A. *Photon. Tech. Lett.* **2**, 234–236 (1990).
21. Schneider, R. P. & Lott, J. A. *Appl. Phys. Lett.* **63**, 917–919 (1993).
22. Gourley, P. L., Biefeld, R. M., Drummond, T. J. & Zipperian, T. E. *SPIE* **792**, 178–188 (1987).
23. Gourley, P. L. *Superlattices & Microstructures* **1**, 227–230 (1985).
24. Yoffe, G. W., Schlom, D. G. & Harris, J. S. Jr. *Appl. Phys. Lett.* **51**, 1876–1878 (1987).
25. Sahlen, O., Olin, U., Masseboeuf, E., Landgren, G. & Rask, M. *Appl. Phys. Lett.* **50**, 1559–1561 (1987).
26. Jewell, J. L., Scherer, A., McCall, S. L., Gossard, A. C. & English, J. H. *Appl. Phys. Lett.* **51**, 94–96 (1987).
27. Lear, K. L., Chalmers, S., Killeen, K. P. & Zolper, J. *Conf. Lasers & Electro-Optics*, paper CTuD2, Baltimore, 1993 (Optical Society of America, Washington DC, 1993).
28. Peters, M. G. et al. *Proc. SPIE OE/LASE*, Vol. 2147 (Los Angeles, 1994).
29. Gourley, P. L. et al. *Appl. Phys. Lett.* **54**, 1209–1211 (1989).
30. Corzine, S. W., Geels, R. S., Scott, J. W., Yan, R.-H. & Coldren, L. A. *IEEE J. Quantum Electron.* **25**, 1513–1524 (1989).
31. Raja, M. Y. A. et al. *IEEE J. Quantum Electron.* **25**, 1513–1522 (1989).
32. Deppe, D. *Appl. Phys. Lett.* **57**, 1721–1723 (1990).
33. Schubert, E. F. et al. *Appl. Phys. Lett.* **61**, 1381–1383 (1992).
34. Osbourn, G. C. et al. in *Principles and Applications of Semiconductor Strained-Layer Superlattices, Semiconductors & Semimetals* Vol. 24 (ed. Dingle, R.) ch. 8 (Academic, London, 1987).
35. Adams, A. R. *Electron. Lett.* **22**, 249–250 (1986).
36. Yablonovitch, E. & Kane, E. O. *J. Lightwave Technol.* **LT-4**, 504–506 (1986).
37. Welch, D. F., Streifer, W., Schaus, C. F., Sun, S. & Gourley, P. L. *Appl. Phys. Lett.* **56**, 10–12 (1990).
38. Gourley, P. L., Lyo, S. K. & Dawson, L. R. *Appl. Phys. Lett.* **54**, 1397–1399 (1989).
39. Gourley, P. L. et al. *Appl. Phys. Lett.* **55**, 2698–2700 (1989).
40. Hasnain, G., Wynn, J. D., Gunapala, S. & Leibenguth, R. E. *Conf. Quantum Electron. & Laser Sci. paper JThA2*, Anaheim, 1992 (Optical Society of America, Washington DC, 1992).
41. Mukherjee, A., Mahbobzadeh, M., Schaus, C. F. & Brueck, S. R. *J. Photon. Tech. Lett.* **2**, 857–859 (1990).
42. Sinclair, M. B., Gourley, P. L., Brennan, T. M., Hammons, B. E. & Dawson, L. R. *Appl. Phys. Lett.* (submitted).
43. Gourley, P. L. *Appl. Phys. Lett.* **57**, 2410–2412 (1990).
44. Karin, H. R. et al. *Appl. Phys. Lett.* **57**, 963–965 (1990).
45. Wiesenfeld, J. M. et al. *Optical Society of America meet.*, paper FW-1 (Albuquerque, 1992).
46. Hadley, G. R. *Opt. Lett.* **15**, 1215–1217 (1990).
47. Orenstein, M., Kapon, E., Stoffel, N. G., Florez, L. & Harbison, J. P. *Conf. Lasers & Electro-Optics*, paper CPDP29-1 (Anaheim, 1990).
48. Yoo, H. J. et al. *Appl. Phys. Lett.* **56**, 1198–1200 (1990).
49. Warren, M. E. et al. *Appl. Phys. Lett.* **61**, 1484–1486 (1992).
50. Gourley, P. L., Warren, M. E., Vawter, G. A., Brennan, T. M. & Hammons, B. E. *Appl. Phys. Lett.* **60**, 2714–2716 (1992).
51. Vakhshoori, D., Wynn, J. D., Zydzik, G. J. & Leibenguth, R. E. *Appl. Phys. Lett.* **62**, 1718–1720 (1993).
52. Kittel, C. in *Introduction to Solid State Physics* 4th edn Advanced Topic A, 695–699 (Wiley, New York, 1971).
53. Yariv, A. & Yeh, P. in *Optical Waves in Crystals* ch. 4 (Wiley, New York, 1984).
54. St. J. Russell, P. J. *Appl. Phys.* **59**, 3344–3356 (1986).
55. St. J. Russell, P. J. *Physics World* 37–42 August 1992.
56. Yablonovitch, E. *Phys. Rev. Lett.* **58**, 2059–2062 (1987).
57. Ho, K. M., Chan, C. T., Soukoulis, C. M. *Phys. Rev. Lett.* **65**, 3152–3155 (1990).
58. John, S. *Physics Today* **44**, 32–32 (1991).
59. Haus, J. W. *J. mod. Optics* **41**, 195–207 (1994).
60. Sözüer, H. S. & Dowling, J. P. *J. mod. Optics* **41**, 231–239 (1994).
61. Robertson, W. et al. *Phys. Rev. Lett.* **68**, 2023–2026 (1992).
62. Özbay, E. et al. *Phys. Rev. Lett.* **64**, 2059–2061 (1994).
63. Ho, K. M., Chan, C. T., Soukoulis, C. M., Biswas, R. & Sigalas, M. *Solid State Commun.* **89**, 413–416 (1994).
64. Meade, R. D., Brommer, K. D., Rappe, A. M. & Joannopoulos, J. D. *Appl. Phys. Lett.* **61**, 495–497 (1992).
65. Villeneuve, P. R. & Piche, M. *Proc. Quantum Electronics Laser Science Conf.* paper QWG6, Anaheim, 1992 (Optical Society of America, Washington DC, 1992).
66. Yamamoto, Y. & Björk, G. J. *Appl. Phys. Japan* **30**, L2039–L2044 (1991).
67. Faist, J., Capasso, F., Sivco, D. L., Sirtori, C., Hutchinson, A. L. & Cho, A. Y. *Science* **264**, 553–556 (1994).
68. Tsu, R. *Nature* **369**, 442–443 (1994).
69. Morgan, R. A. *Proc. SPIE OE/LASE Conf.*, Los Angeles, 1994 (Society of Photo-instrumentation, Bellingham, Washington DC, 1994).

ACKNOWLEDGEMENTS. I thank colleagues at Sandia National Laboratories who have collaborated on microstructured lasers and materials, including T. Brennan, W. Chow, R. Dawson, T. Drummond, G. Hammons, R. Hadley, K. Lear, A. McDonald, R. Schneider, M. Sinclair, A. Vawter, M. Warren, J. Wendt & T. Zipperian. I also thank R. Slusher of AT&T Bell Laboratories and R. Morgan of Honeywell for supplying photographs of Fig. 5 and Fig. 6, respectively. The work was supported in part by the Department of Energy and the Office of Basic Energy Sciences.